THE JOURNAL OF PHYSICAL CHEMISTRY C

Article

pubs.acs.org/JPCC

A Simple Kinetic Model for Singlet Fission: A Role of Electronic and Entropic Contributions to Macroscopic Rates

Anatoly B. Kolomeisky,*[,†] Xintian Feng,[‡] and Anna I. Krylov*[,‡]

[†]Department of Chemistry, Rice University, Houston, Texas 77251-1892, United States

[‡]Department of Chemistry, University of Southern California, Los Angeles, California 90089-0482, United States

ABSTRACT: A simple three-state model for the dynamics of the singlet fission (SF) process is developed. The model facilitates the analysis of the relative significance of different factors, such as electronic energies, couplings, and the entropic contributions. The entropic contributions to the rates are important; they drive the SF process in endoergic cases (such as tetracene). The anticipated magnitude of entropic contributions is illustrated by simple calculations. By considering a series of three acenes (tetracene, pentacene, and hexacene), we explained the experimentally observed 3 orders of magnitude difference in the rate of SF in tetracene and pentacene and predicted that the rate in hexacene will be slightly faster than in pentacene. This trend is driven by the increased thermodynamic drive for SF (Gibbs free energy difference of the initial excitonic state and two separated triplets). The model also explains experimentally observed fast SF in 5,12-diphenyltetracene. Consistently with the experimental observations, the model predicts weak temperature dependence of the multiexciton formation rate in tetracene as well as a reduced rate of this step in solutions and in isolated dimers.

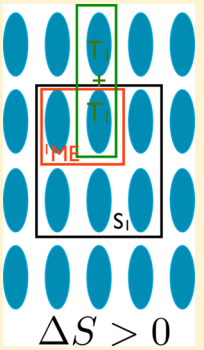

1. INTRODUCTION

Singlet fission (SF) is a nonadiabatic process in which one singlet excited state splits into two triplets that ultimately give rise to four charge carriers.[1] If this process is harnessed in solar cells, their efficiency can be increased beyond the Shockley–Queisser limit by efficiently utilizing higher-energy photons. Although this phenomenon was discovered a long time ago,[2] its mechanistic understanding is incomplete, which hinders the design of organic photovoltaic materials for solar energy conversion. Recent reviews[1,3] summarize experimental and theoretical work investigating the mechanisms of SF in molecular solids and model compounds.

The electronic structure aspects of SF have received considerable attention.[1,3−12] The important quantities are energy levels (lowest bright singlet states of individual chromophores should be about twice higher than T_1) and electronic couplings between an initial excitonic state and a dark multiexciton state that eventually splits into two independent triplets. These factors depend strongly on the relative orientations of the individual molecules,[4,13] which is likely to be responsible for observed effects of morphology on the rates and yields of SF.

One can connect the rates and electronic quantities by modeling complicated nonadiabatic dynamics encompassing several interacting electronic states. Simple estimates can be obtained using the Landau–Zener type of approaches.[7] Two studies[14,15] presented calculations aiming at complete macroscopic description of the SF process from first-principles employing approximate electronic structure models. In stark contrast to the large number of electronic structure studies, only recently has a possible role of entropy in promoting SF been noted.[16]

Phenomenological kinetic models of SF and a reverse process, triplet–triplet annihilation, have been developed, with an emphasis on explaining magnetic field effects.[17,18] Kinetic models of varying complexity are often employed in analyzing the experimental data.[16,19−22]

Our motivation is to develop a simple kinetic model that will allow us to connect electronic structure calculations with the experimental observables. We aim at establishing a theoretical framework that will explain the observed trends in SF yield and, more importantly, enable screening of various structures with respect to their efficiency in performing SF.

In our previous work,[13] we discussed essential features of the underlying electronic structure and calculations of quantities relevant to SF process. We frame the discussion in terms of correlated many-electron adiabatic states that are coupled by nonadiabatic (derivative) couplings. The electronic states involved are an initially excited bright singlet state (of a mixed excitonic and charge-resonance character), a dark singlet multiexciton (or biexciton) state (ME or ^{1}(TT), two singlet-coupled triplets with a variable admixture of charge-resonance configurations) coupled to the singlet state by a nonadiabatic coupling, and two independent triplets (T_1+T_1) that lost their coherence.

The most basic quantity relevant to SF is the electronic energy difference between the initially excited singlet state and twice the energy of separated triplets:

$$E_{\mathrm{stt}} = E[\mathrm{S}_1] - 2 \times E[\mathrm{T}_1] \quad (1)$$

Received: December 31, 2013
Revised: February 4, 2014
Published: February 14, 2014

dx.doi.org/10.1021/jp4128176 | J. Phys. Chem. C 2014, 118, 5188–5195

For efficient solar energy conversion, these two states should be approximately isoenergetic, the small electronic energy mismatch being compensated by vibrational motion. In pentacene, $E_{stt} > 0$, and the overall SF process is exoergic, however, in tetracene $2 \times E_T > E_S$. The rate of electronic transition from the bright singlet state to ^{1}ME is proportional to nonadiabatic coupling, which is related to the norm of the one-electron transition density matrix, $\|\gamma\|$. The third important quantity is multiexciton stabilization (or binding) energy, E_b, that we define as the energy difference between the ^{1}ME and ^{5}ME states (the former is stabilized by configuration interaction with other singlet configurations, whereas the latter maintains pure diabatic character of two entangled triplets). Because fission results in a loss of decoherence yielding two independent triplets, E_b can be interpreted as a minimal energy required for the separation of two triplets to occur. Although E_{stt} is dominated by the S_1 and T_1 excitation energies of the isolated monomers, it is also affected by Davydov's splitting and, therefore, can be modulated by local environment. $\|\gamma\|$ and E_b are also sensitive to the local environment. Thus, all three quantities can be tuned by structural modifications of the chromophores affecting their packing. Table 1 summarizes

Table 1. Electronic Energies (eV) in Tetracene, Pentacene, and Hexacene[a]

system	E_{stt} (monomer[b])	E_{stt} (bulk[c])	E_{stt} (exp)	E_b[d]
tetracene	−0.342	−0.303	−0.18[e]	0.028
pentacene	0.281	0.245	0.21[e]	0.038
hexacene	0.803	0.625	0.74[f]/0.32[g]	0.049

[a]See ref 13 for details of the computational protocol. [b]SOS-CIS(D) values. [c]Computed for the AB dimer as $E[S_1(AB)] - E[^5ME(AB)]$ by using corrected RAS-2SF values. [d]RAS-2SF values for AB dimer computed as $E[^5ME] - E[^1ME]$. [e]From ref 1. [f]Solution (ref 23). [g]Film (ref 24).

relevant electronic energies for tetracene, pentacene, and hexacene. We note that calculations of E_{stt} involve larger error bars than calculations of E_b, due to error cancelation (the two ME states have the same character; thus, the dynamic correlation effects are quite similar and cancel out).

While most electronic structure studies have been focusing on characterizing relevant electronic energies and couplings, one needs to operate with Gibbs free energies to understand driving forces in the SF process and to compute rates. There is a thermodynamic driving force if the overall change in the free energy is negative, even if electronic energy differences are unfavorable (as, for example, in tetracene). The structure of molecular solids, such as packing, can affect the free energies of each state via entropic contributions. A possible role of entropy has been recently emphasized by Zhu and co-workers.[16] In this paper, we discuss calculations of the entropic contributions using a minimal kinetic model for SF that captures the essential physics of the process. The model explains the observed difference in the SF rate between tetracene, pentacene, and 5,12-diphenyltetracene (DPT) and makes a prediction about hexacene. Consistently with experimental observations, the model predicts weak temperature dependence of the ME formation rate in tetracene as well as a reduced rate of this step in solutions and in isolated dimers.

The structure of the paper is as follows. Section 2 presents the kinetic model, section 3 describes calculations of entropic contributions, and section 4 presents the discussion.

2. KINETIC MODEL FOR THE SF PROCESS

Singlet fission is a complex process encompassing many states. Our goal is not to take into account all microscopic details but rather to develop a simple conceptual picture of the process that would provide a semiquantitative description of dynamics; thus, we choose the minimalist kinetic scheme that has only three states. It means that many states are combined into these three states.

Figure 1 shows the energy diagram for such a minimal three-state model (see Table 1 for electronic energies). We assume

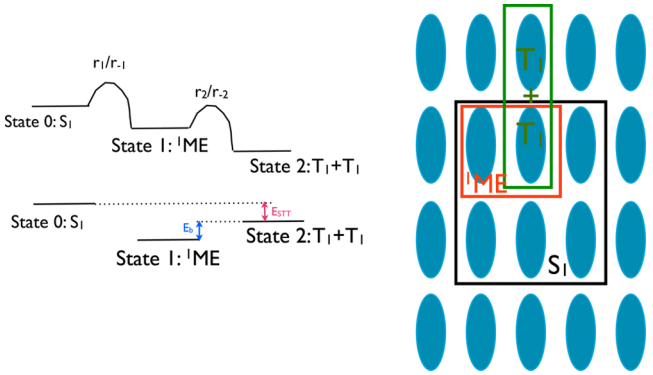

Figure 1. Three-state model of singlet fission. Top left: free energies of the initially excited bright (S_1, denoted as "state 0"), multiexciton singlet (^{1}ME, denoted as "state 1"), and two uncoupled triplets (T_1+T_1, denoted as "state 2"). Bottom left: Electronic energy diagram. In pentacene, state 2 is lower than state 0 ($E_{stt} > 0$). In tetracene, it is slightly above ($E_{stt} < 0$). Thus, $E_0 = 0$, $E_1 = -E_{stt} - E_b$, and $E_2 = -E_{stt}$. Right: Cartoon illustrating the nature of S_1, ^{1}ME, and T_1+T_1 that gives rise to entropic contributions. State 0 is delocalized over several chromophores (black rectangle). The ME state can be localized on any pair of adjacent molecules (red rectangle) within the initial exciton. Our model assumes that triplet separation (second step) occurs when one of the triplet excitons hops to another chromophore (green rectangle).

that the process begins with populating the bright state (denoted by state 0). The second step is population of the multiexciton state (state 1); the rates for the forward and backward reactions are denoted as r_1 and r_{-1}, respectively. The third step is the production of independent triplets (state 2); the forward and backward rates are r_2 and r_{-2}. We choose to frame our discussion in terms of rates rather than rate constants (k_1/k_{-1} and k_2/k_{-2}) to account for possible concentration effects and to simplify the calculation of characteristic times for SF. In a single-molecule framework employed here, the rates are identical to the respective rate constants (i.e., one can rewrite all the equations using k's instead of r's); however, the situation in solutions is different, and the rates should include both rate constants and the respective concentrations. Thus, our formulation is appropriate both for molecular solids and for solutions.

Using a linear free energy argument,[25] the rates are related to the free energies of the three states (see Figure 1):

$$G_0 = 0 \tag{2}$$

$$G_1 = -E_{stt} - E_b - TS_1 = -\epsilon_{stt} - \epsilon_b \tag{3}$$

$$G_2 = -E_{stt} - TS_2 = -\epsilon_{stt} \tag{4}$$

where electronic energies are computed relative to state 0 and the calculations of respective entropic contributions are

dx.doi.org/10.1021/jp4128176 | J. Phys. Chem. C 2014, 118, 5188−5195

described in section 3. ϵ_{stt} and ϵ_b are now free energy differences that incorporate both electronic and entropic contributions:

$$\epsilon_{stt} = E_{stt} + TS_2 \tag{5}$$

$$\epsilon_b = E_b + TS_1 - TS_2 \tag{6}$$

$-\epsilon_{stt}$ characterizes overall driving force for SF, whereas ϵ_b is multiexciton stabilization (or binding) free energy. Relevant free energy differences are:

$$\Delta G \equiv G_2 - G_0 = -\epsilon_{stt} \tag{7}$$

$$\Delta G_1 \equiv G_1 - G_0 = -\epsilon_{stt} - \epsilon_b \tag{8}$$

$$\Delta G_2 \equiv G_2 - G_1 = \epsilon_b \tag{9}$$

For the SF process to be thermodynamically possible, the total Gibbs free energy change, ΔG, should be negative, which means that ϵ_{stt} must be positive. As one can see from eq 5, negative E_{stt} (endoergic SF) can be surpassed by sufficiently large entropic gain in state 2. ΔG_1 or ΔG_2 may, in principle, be positive, provided that $\Delta G < 0$. However, a large positive value for either ΔG_1 or ΔG_2 would mean that the respective step is too slow for the overall process to happen on a realistic time scale, even though the overall reaction is thermodynamically allowed (just like diamonds-to-graphite transition). For example, positive ME stabilization free energy, as defined in eq 6, will slow down the second step. ϵ_b depends on the difference of entropic terms for state 1 (bound multiexciton state) and state 2 (two independent triplets), and negative values mean that the ^{1}ME state is unbound and the second step is fast.

The quantity of interest is the total time τ to reach state 2. It can be computed as a first-passage time, a powerful theoretical tool that was widely used in many chemical, physical, and biological processes:[26]

$$\begin{aligned}\tau &= \frac{1}{r_1} + \frac{1}{r_2} + \frac{r_{-1}}{r_1 r_2} \\ &= \frac{1}{r_1} + \frac{1}{r_2} + \frac{1}{K_1^{eq} r_2} \\ &= \frac{1}{r_1} + \frac{1}{r_2}\left(1 + \frac{1}{K_1^{eq}}\right)\end{aligned} \tag{10}$$

where K_1^{eq} is an equilibrium constant for step 1. As one can see, when $K_1^{eq} \gg 1$, the total time is just the sum of the inverses of individual rates. However, if K_1^{eq} is small, the relative contribution of step 2 into the total time becomes more pronounced.

Efficient SF will be identified by small τ. Thus, our aim is to investigate the dependence of τ on E_{stt}, γ, and E_b, as well as entropic factors for the three states. We note that this model aims to describe the efficiency of the initial SF steps and will not be able to describe long-time (nanosecond) kinetics that involves diffusion, trapping, and recombination of independent triplet excitons.[19] The model is not suitable for describing magnetic field effects on SF.[17] However, this theoretical framework can be extended to take these processes into account.

The ratios of forward and backward rates are determined by free energy differences satisfying the detailed balance condition:

$$\frac{r_1}{r_{-1}} = \exp[\beta(G_0 - G_1)] = \exp[\beta(\epsilon_{stt} + \epsilon_b)] \tag{11}$$

$$\frac{r_2}{r_{-2}} = \exp[\beta(G_1 - G_2)] = \exp[\beta(-\epsilon_b)] \tag{12}$$

where $\beta = 1/k_B T$. Absolute rates depend on respective activation energies and prefactors. It is convenient to write down the expressions for absolute rates as following:

$$r_1 = r_1(0)\exp[\theta\beta\epsilon_b] \tag{13}$$

$$r_{-1} = r_{-1}(0)\exp[(\theta - 1)\beta\epsilon_b] \tag{14}$$

$$r_2 = r_2(0)\exp[-\theta\beta\epsilon_b] \tag{15}$$

$$r_{-2} = r_{-2}(0)\exp[(1 - \theta)\beta\epsilon_b] \tag{16}$$

In these equations, rates $r_i(0)$ ($i = 1, -1, 2, -2$) correspond to a *hypothetical* case when the ME stabilization energy is zero ($\epsilon_b = 0$). This procedure chooses a zero energy, and it is done for convenience only. Our calculations obviously do not depend on the choice of the reference state. In addition, parameter $0 \le \theta \le 1$ describes the relative position of the transition state along the reaction coordinate, e.g., for $\theta = 1/2$; the transition state is halfway between the reactants and products. For simplicity, we assumed that θ is the same for both steps. This approach allows us to analyze the effect of local structure by focusing on ϵ_b.

Thus, all information about activation energies and prefactors is now contained in $r_i(0)$. We note that the detailed balance condition requires that:

$$\frac{r_1(0)}{r_{-1}(0)} = \exp(\beta\epsilon_{stt}) \tag{17}$$

Using Fermi Golden Rule and the analysis in ref 13, one could argue that rates $r_1(0)$ and $r_{-1}(0)$ are proportional to $\|\gamma\|^2$ (or, more precisely, to $\|\gamma\|^2/(E_{stt} + E_b)^2$) that describes the coupling between S_1 and ^{1}ME. Strong coupling would correspond to fast rates in both directions and relatively weak dependence on the temperature, while in the case of weak coupling these rates are small and strongly temperature-dependent. Transition rates $r_2(0)$ and $r_{-2}(0)$ describe Dexter energy transfer between perfectly isoenergetic chromophores ($\epsilon_b = 0$); they fall off quickly with distance (it is generally assumed that Dexter transfer is operational within 10−20 Å). One can anticipate that $r_2(0)$ and $r_{-2}(0)$ would be very similar in homologous compounds that share similar structure (e.g., crystalline tetracene and pentacene).

The explicit expressions for transition rates allow us to estimate the average times for the SF process:

$$\begin{aligned}\tau = &\frac{\exp[-\theta\beta\epsilon_b]}{r_1(0)} + \frac{\exp[\theta\beta\epsilon_b]}{r_2(0)} \\ &+ \frac{\exp[(\theta - 1)\beta\epsilon_b] r_{-1}(0)}{r_1(0) r_2(0)}\end{aligned} \tag{18}$$

Analysis of eq 18 suggests that there is an optimal value for ϵ_b at which the singlet fission is the fastest. A more positive ME stabilization energy lowers the first and third terms, while it also increases the second term. Physically it means that for large and positive ϵ_b (bound ME state), the first transition (from state 0 to state 1) is faster, while the second transition (from state 1 to state 2) is getting slower, suggesting that there is some optimal value of the multiexciton stabilization energy. Similar arguments

dx.doi.org/10.1021/jp4128176 | J. Phys. Chem. C 2014, 118, 5188−5195

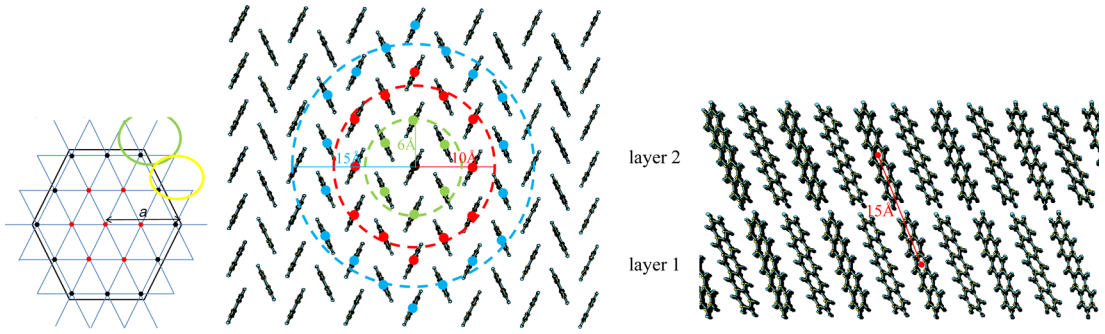

Figure 2. Crystal structure of tetracene and pentacene. Molecular arrangement in the *ab* plane (left and center) and in perpendicular direction (right).

can be made for negative ϵ_b (unbound ME); a more negative value would impede the first step but speed up the second. The optimal condition for ϵ_b can be easily obtained by taking a derivative of τ with respect to the total binding energy. To illustrate this, let us assume that $\theta = 1/2$. Then by minimizing the time for SF with respect to the total binding energy, we obtain:

$$x^2 = \frac{r_2(0)}{r_1(0)} + \frac{r_{-1}(0)}{r_1(0)} \tag{19}$$

where we defined an auxiliary function:

$$x = \exp\left(\frac{\beta\epsilon_b}{2}\right) \tag{20}$$

Solving eq 19 yields the prediction for the optimal binding energy in terms of transition rates $r_i(0)$:

$$\epsilon_b^* = k_B T \ln\left[\frac{r_2(0)}{r_1(0)} + \frac{r_{-1}(0)}{r_1(0)}\right] = -\epsilon_{stt} + k_B T \ln\left[\frac{r_2(0)}{r_1(0)}\right] \tag{21}$$

We note that, unlike the overall rate, the value of optimal ϵ_b depends strongly on the free energy landscape, i.e., the value of parameter θ. By choosing $\theta = 1$ instead of 0.5, the minimization of eq 18 yields:

$$x^4 = \frac{r_2(0)}{r_1(0)} \tag{22}$$

instead of eq 19, giving rise to the optimal value of ϵ_b that does not depend on ϵ_{stt}:

$$\epsilon_b^* = \frac{k_B T}{2} \ln\left[\frac{r_2(0)}{r_1(0)}\right] \tag{23}$$

Let us now analyze eqs 21 and 23. The second term in eq 21 is the same (up to a factor of 2) as eq 23. When $r_2(0) > r_1(0)$, this term is positive. Thus, in the case of $\theta = 1$ (transition state on the product side), optimal ϵ_b is positive; larger $r_2(0)$ mean more positive values. This can be easily rationalized by analyzing eq 18: large $r_2(0)$ will reduce the magnitude of the second term, while positive ϵ_b will make the first term smaller (the third term is zero for $\theta = 1$). Consequently, if $r_2(0) < r_1(0)$, negative ϵ_b (unbound ME) is desired. If $r_1(0) = r_2(0)$, then the optimal value for ϵ_b is zero; this means that the overall rate for the first step, r_1, should be equal to r_2 to achieve the shortest τ.

In the case of $\theta = 0.5$ (transition state between the reactants and products), optimal ϵ_b depends on ϵ_{stt}. For example, if $r_2(0) \approx r_1(0)$, then:

$$\epsilon_b^* \approx -\epsilon_{stt} \tag{24}$$

First, we note that in this case ϵ_b is negative (unbound multiexciton). Thus, if overall thermodynamic driving force for SF is large, then fastest rates are achieved at relatively large and negative multiexciton stabilization energies. However, for small ϵ_{stt}, ϵ_b should be less negative, to make the first step sufficiently fast. The effect of the second term is exactly as in the case of $\theta = 1$, if $r_2(0) \gg r_1(0)$, more positive ϵ_b is required to achieve optimal rate by speeding the first step.

For another limiting case of $\theta = 0$, one can show that the optimal ME stabilization energy must be very large and positive. For all other cases, the optimal ME stabilization energy can be understood by interpolating between the three limiting behaviors explained above.

3. ENTROPY CALCULATIONS

Below we provide an illustrative calculation of entropic contributions. As will become evident, the calculation invokes several assumptions; thus, it is of a semiquantitative value. To estimate relative entropic contributions, we rely on the following simple reasoning (similar to that of ref 16). As illustrated in Figure 1, state 0 is delocalized[7,8] (or effectively delocalized owing to the ultrafast exciton hopping[14]); however, state 1 is localized on two neighboring chromophores. Thus, to estimate entropy of state 1, one needs to count by how many ways one can choose a pair of neighboring chromophores from the initially prepared delocalized exciton. In state 2, two triplets are separated; thus, the entropic contribution can be estimated by counting a number of ways in which a multiexciton state can separate within the Dexter radius.

In polycrystalline materials, the initial exciton is delocalized, as evidenced by the noticeable spectral shift (relative to solution) and also supported by electronic structure calculations.[7,8] The most thorough study of exciton delocalization is presented in ref 8 where it was found that low-lying singlet excited states exhibit an average electron−hole distance greater than 6 Å. From the figures visualizing the exciton, the exciton appears to be delocalized over about 13 molecules (in pentacene). Also, in agreement with molecular orbital considerations, the delocalization is most prominent in the *ab* plane.

Figure 2 shows crystal structure of solid pentacene (tetracene is very similar, except for interlayer distance). In the *ab* plane, each molecule has six nearest neighbors. The average distance

dx.doi.org/10.1021/jp4128176 | J. Phys. Chem. C 2014, 118, 5188−5195

between the chromophores in the *ab* plane is similar for tetracene and pentacene and is about 6 Å. The distance between the planes is 15 Å in pentacene (and is shorter in tetracene).

We assume that both steps of SF occur in the *ab* plane. We begin by calculating the number of chromophore molecules, N, contained in n coordination shells. Because the ith coordination shell adds $6i$ molecules, then

$$N = 3n^2 + 3n + 1 \tag{25}$$

Using the distance between the chromophores centers, n can easily be connected with a spatial extent.

To estimate entropic contribution to state 1, we compute the number of unique adjacent chromophore pairs within n coordination shells. As one can see from Figure 2, the total number of possible pairs for one molecule is 6 (the number of edges that connect it to the nearest neighbors). Therefore, $6N$ is the total number of pairs in which the edges inside the black hexagon are counted twice. The number of edges that are outside the black hexagon is $P_s^+ = 3 \times 6 + 2 \times (N_s - 6) = 12n + 6$, where we have 6 points that have 3 outer edges, and the rest $(N_s - 6)$ have 2 outer edges. P_s^+ is counted only once, so the total number of edges $P = (6N + P_s^+)/2$. Thus, the total number of pairs is:

$$\Omega_1 = 9n^2 + 15n + 6 \tag{26}$$

To estimate entropy for state 2, we consider the number of ways that a triplet exciton can hop within the area determined by the Dexter radius. Let N_t denote the number of molecules within the Dexter radius (10−20 Å) that comprises n shells. Then

$$\Omega_2 = \frac{N_t(N_t - 1)}{2} \times 2 = (3n^2 + 3n + 1)(3n^2 + 3n) \tag{27}$$

Here the factor of 2 accounts for the two triplets formed from one ME state. We note that Ω_2 depends quadratically on the number of molecules within the Dexter radius, whereas Ω_1 depends linearly on the number of molecules covered by the singlet exciton delocalization. This is important because for the second step to be thermodynamically favorable, Ω_2 should be greater than Ω_1 (E_b is positive; see Table 1). We note that if the ^{1}ME state is mobile and can hop, this will contribute toward increasing the effective radius and, therefore, increase Ω_2.

Table 2 collects the results of entropic contributions for states 1 and 2 as a function of the number of coordination shells (we note that, in general, n should be different for state 1 and state 2 because of differences in the underlying physical processes).

Table 2. Entropic Contributions as a Function of the Number of Coordination Shells

n	R, Å	N	Ω_1[a]	Ω_2[b]	TS_1, eV[c]	TS_2, eV[c]
1	6	7	30	42	0.088	0.096
2	10	19	72	342	0.110	0.150
3	15	37	132	1332	0.125	0.185
4	20	61	210	3660	0.137	0.211
5	25	91	306	8190	0.147	0.231
6	30	127	420	16002	0.155	0.249

[a]Using eq 26. [b]Using eq 27. [c]$k_B = 8.6173 \times 10^{-5}$ eV/K; $k_BT = 0.026$ eV at 298 K.

4. DISCUSSION

We begin by analyzing the thermodynamic driving force for the overall SF process. Clearly, the entropic contribution is always beneficial for SF ($TS_2 > 0$). We note that such entropic contributions depend critically on the concentration of chromophore molecules; thus, they will not be operational in dilute solutions, which is partially responsible for low SF yields in isolated covalently linked dimers.[1,27] We note that in a recent study efficient SF has been reported in pentacene solutions;[28] the kinetics revealed that the process is diffusion-limited, and the yield shows a strong concentration dependence. Whereas it is not surprising that the overall process occurs on a nanosecond time scale (time required for an excited chromophore to find another one to form an excimer, a solution analog of state 0), the kinetics of the ME formation (step 1 in our model) is 3 orders of magnitude slower than in solid pentacene (ref 28 reports 400−530 ps).

On the basis of the results collected in Table 2, and taking 10−25 Å as a radius within which triplet separation may occur, we expect values of ≈0.2 eV, which is sufficient to make SF in tetracene possible. We note that the minimal number of shells required to make $\Delta G < 0$ (in tetracene) is 3 (corresponding to $TS_2 = 0.185$ eV). In pentacene, entropic contributions increase the driving force for SF. We note that possible mobility of the ^{1}ME state and/or triplet separation between the planes will further increase this value.

Despite large uncertainties involved in calculations of entropic contributions, only limited variations in TS_1 are possible. TS_2 has a lower bound determined by endothermicity of SF in tetracene. ΔG_2 or ΔG_1 may, in principle, be positive; however, too large positive values would make individual steps too slow for the process to occur on a realistic time scale. Thus, we first consider the range of TS_1 that would result in $\Delta G_2 < 0$ and $\Delta G_1 > 0$.

Equation 9 means that the entropic contributions should make the multiexciton unbound, to promote triplet separation. Using $TS_2 = 0.185$ eV, $\Delta G_2 < 0$, but $\Delta G_1 < 0$. Using $TS_2 = 0.211$ eV ($n = 4$) or 0.231 eV ($n = 5$), both conditions can be satisfied with $TS_1 = 0.155$ eV ($n = 6$). The resulting thermodynamic quantities for these two combinations of TS_1 and TS_2 are summarized in Table 3.

To consider the case when $\Delta G_2 < 0$ and $\Delta G_1 > 0$ (corresponding to a small yield of ^{1}ME), we also performed calculations for $TS_2 = 0.211$ eV ($n = 4$) and $TS_1 = 0.147$ eV ($n = 5$), as well as $TS_2 = 0.185$ eV ($n = 3$) and $TS_1 = 0.147$ eV ($n = 5$). The results of these two calculations, which correspond to smaller efficient delocalization of S_1, are also given in Table 3.

Let us now analyze eq 18 in more detail. As illustrated by Table 3, the calculated ϵ_b are very similar in all three compounds; consequently, the values of $\exp(0.5\beta\epsilon_b)$ are also very close. Using ϵ_b computed with $TS_1 = 0.147$ eV and $TS_2 = 0.211$ eV, we arrive at the following:

$$\tau^t = \frac{2.05}{r_1^t(0)} + \frac{1.11}{r_2^t(0)} \tag{28}$$

$$\tau^p = \frac{1.65}{r_1^p(0)} + \frac{0.61}{r_2^p(0)} \tag{29}$$

$$\tau^h = \frac{1.33}{r_1^h(0)} + \frac{0.75}{r_2^h(0)} \tag{30}$$

dx.doi.org/10.1021/jp4128176 | J. Phys. Chem. C 2014, 118, 5188−5195

Table 3. Relevant Thermodynamic Quantities (eV) in Tetracene, Pentacene, and Hexacene[a] at 298 K

	ϵ_{stt}	ϵ_b	ϵ_b^* [b] ($\theta = 0.5$)	ϵ_b^* ($\theta = 1$)
$TS_1 = 0.155$ and $TS_2 = 0.211$				
tetracene	0.031	−0.028	0.147	0.089
pentacene	0.421	−0.018	−0.423	0.001
hexacene	0.531	−0.007	−0.571	−0.020
$TS_1 = 0.155$ and $TS_2 = 0.231$				
tetracene	0.052	−0.048	0.126	0.089
pentacene	0.441	−0.038	−0.443	0.001
hexacene	0.551	−0.027	−0.592	−0.020
$TS_1 = 0.147$ and $TS_2 = 0.211$				
tetracene	0.031	−0.036	0.147	0.089
pentacene	0.421	−0.026	−0.423	0.001
hexacene	0.531	−0.015	−0.571	−0.020
$TS_1 = 0.147$ and $TS_2 = 0.185$				
tetracene	0.005	−0.010	0.173	0.089
pentacene	0.395	0.0002	−0.397	0.001
hexacene	0.505	0.011	−0.545	−0.020

[a]Computed using experimental E_{stt}; see Table 1. [b]ϵ_b^* is computed using eqs 21 and 23 and the same parameters as in the rate calculations.

A reasonable assumption is that $r_2(0)$ is very similar in all acenes (and is probably fast compared to $r_1(0)$, at least in tetracene). Thus, 3 orders of magnitude difference in the rates of SF in tetracene and pentacene should be due to the respective $r_1(0)$. Using a linear free energy approach,[25] which argues that the activation energy for a process is proportional to the free energy difference of the reaction, one can write:

$$r_1(0) \sim \exp(\alpha\beta\epsilon_{stt}) \tag{31}$$

where α is a coefficient determining the relationship between E_a and ΔG. We note that within this approach $r_2(0)$ should be the same for the three compounds, as it is defined as a hypothetical rate when $\epsilon_b = 0$. To account for variations in coupling, we multiply $r_1(0)$ by the respective $\|\gamma\|^2/(E_{stt} + E_b)$; $\|\gamma\|^2$ equals 0.115, 0.166, and 0.193 for tetracene, pentacene, and hexacene, respectively. Using $\alpha = 0.5$ and the computed E_{stt}, E_b, and $\|\gamma\|^2$, we obtain:

$$r_1^t(0) : r_1^p(0) : r_1^h(0) = 1 : 1077 : 4814 \tag{32}$$

Note that because we use the same entropic factors for all three compounds, these ratios are determined by E_{stt}, E_b, and $\|\gamma\|^2$ alone and, therefore, do not depend on the specific choices of TS_1 and TS_2 (but they do depend on T).

By taking $r_1^t(0) \approx 10^{10}$ s^{-1} and $r_2(0) \approx 10^{13}$ s^{-1}, one can explain the experimentally observed difference[1,27] between tetracene and pentacene, and to make a prediction about hexacene:

$$\tau^t \approx 201 \text{ ps} \tag{33}$$

$$\tau^p \approx 214 \text{ fs} \tag{34}$$

$$\tau^h \approx 103 \text{ fs} \tag{35}$$

The computed times for different choices of TS_1 and TS_2 are summarized in Table 4. As these results demonstrate, the computed times are quite robust within the reasonable range of variations of TS_1 and TS_2. We also note that variations of θ have negligible effect on computed τ.

These simple calculations suggest that:

Table 4. Computed Characteristic Times for Tetracene, Pentacene, and Hexacene

TS_1, eV	TS_2, eV	τ^t, ps	τ^p, fs	τ^h, fs
0.155	0.211	171	202	112
0.155	0.231	256	243	94
0.147	0.211	201	214	103
0.147	0.185	121	192	141

- The first step is rate-determining in tetracene; it becomes much faster in pentacene and hexacene due to increased thermodynamic driving force (ϵ_{stt}) for the SF process.
- One can expect that already in pentacene the rates of step 1 and step 2 might become comparable.
- Within our simple model, the rate of the first step in hexacene becomes very fast; thus, we expect that the second state might become rate-limiting.
- We expect that the rate of SF in hexacene will be comparable (yet slightly faster) to that in pentacene.
- Computed $\|\gamma\|^2$ are very similar in all three compounds; thus, the relative strength of couplings is unlikely to be responsible for very different rates of SF in tetracene and in pentacene.

Of course, the presented calculations should be regarded as of qualitative value, owing to the simplicity of the model and numerous assumptions. Yet, they present a framework for analyzing the growing data on the kinetics and yields of SF in various systems. Moreover, they highlight the relative significance of different factors (singlet−triplet energy gaps, entropic factors, and couplings) for the overall rate of SF.

Using the above values of $r_1(0)$ and $r_2(0)$, we compare the computed ϵ_b with the optimal values, as predicted by eq 21. The results for $\theta = 0.5$ and $\theta = 1$ are summarized in Table 3. We note that in tetracene, optimal ϵ_b is positive, consistently with a very slow first step owing to a small thermodynamic drive due to small ϵ_{stt}. One can easily see that while the calculations of rates are relatively insensitive to the value of parameter θ that characterizes the free energy landscape, the optimal value of ϵ_b is strongly θ-dependent. When using $\theta = 0.5$, ϵ_b^* are 1−2 orders of magnitude larger than the actual ϵ_b. When using $\theta = 1$ (transition state at the product side), the computed optimal multiexciton stabilization energies (using eq 23) are 0.089 eV, 0.001 eV, and −0.020 eV for tetracene, pentacene, and hexacene, respectively; these values are much closer to the actual ϵ_b. Without more detailed knowledge of the free energy surface, it is unclear whether these systems are close to the optimal state.

To further test our model, we estimated the rate of SF in DPT; this material shows very efficient SF, with fast and slow rate components of 1.3 and 105 ps, respectively.[19] We employ $TS_1 = 0.147$ eV and $TS_2 = 0.211$ eV. Admittedly, this is a very crude estimate, as one may expect that the entropic contributions in an amorphous solid could be rather different. While the physical nature of excitons in amorphous solids is different from crystalline materials, simple estimates suggest that their effective radius of delocalization (for the purpose of counting microstates in entropy calculations) may be similar. The spectra of solid DPT and DPT in solutions are identical[19] indicating the localized nature of the initial exciton. However, as shown by the ab initio molecular dynamics simulations,[14] the initially excited state in DPT hops around frequently (about once per 100 fs), giving rise to effective delocalization (for the purpose of calculating entropic contributions), i.e., in the

dx.doi.org/10.1021/jp4128176 | J. Phys. Chem. C 2014, 118, 5188−5195

course of 1 ps, the exciton will cover a sphere of the radius of about 20 Å, which is indeed very close to the exciton size in tetracene and pentacene.

Using experimental E_{stt} = 0.08 eV and computed (using the same protocol) E_b = 0.022 eV and $\|\gamma\|^2$ = 0.140, we arrive at τ^{DPT} = 0.6 ps, which is in a semiquantitative agreement with the experimental trend. On the basis of our model, efficient SF in DPT can be attributed to an improved energy gap (E_{stt}) which increases thermodynamic drive and also increased coupling.

Using our estimates of the entropic terms, we evaluate anticipated differences in the rate of the first step, r_1, for covalently linked dimers or in solutions (assuming that an excimer-like dimer is already formed). Assuming that all electronic factors (E_{stt}, E_b, and $\|\gamma\|^2$) are the same in the dimers as in the respective solids (which is of course a rather crude approximation), the ratio is (using the linear free energy approach and α = 0.5):

$$r_1^{dimer}: r_1^{solid} = \exp[-0.5\beta(TS_1)] \approx 0.03-0.05 \quad (36)$$

Thus, due to the entropic factors alone, the dimers (either covalently linked or excimers formed in solutions) are expected to exhibit $S_1 \rightarrow$ ME rates that are about 20−30 times slower than in respective pristine solids. Of course, to evaluate the actual rates, one should also take into account changes in the electronic factors. When applied to covalently linked dimers from ref 27, our model reproduces the observed 3 orders of magnitude drop in SF rates; the analysis of different components reveals that both electronic (couplings, variations in energies) and entropic factors are important.

As a final remark, our model predicts a very weak temperature dependence of the first step, $S_1 \rightarrow$ ME, in tetracene. Using the same parameters as in the rate calculations above (and Ω_1 = 306 and Ω_2 = 3660; see Table 2), the model predicts that the characteristic time of the first step in tetracene will increase only by a factor of 2 when the temperature is lowered by 100 K. The second step, however, is more sensitive, and the respective time will increase by a factor of 15. These results are in qualitative agreement with recent experimental observations.[29,30] The weak dependence can be easily rationalized by writing the rate as:

$$r \sim \exp\left(-\frac{\alpha\Delta G}{k_B T}\right) = \exp\left(\alpha\frac{\Delta S}{k_B}\right)\exp\left(-\alpha\frac{\Delta E}{k_B T}\right) \quad (37)$$

Thus, when electronically a reaction is nearly isoergic ($\Delta E \approx 0$), the relative importance of the temperature-dependent second term is small. In our calculation, we assumed that exciton delocalization is not affected by temperature. However, at low temperatures, superradiant emission from tetracene has been reported by Bardeen and co-workers[31] and attributed to an increase in the coherence length. Thus, one may expect an increase of exciton delocalization that will enhance the relative importance of the entropic contribution. This would result in reducing the temperature dependence even further.

5. CONCLUSIONS

We employed a simple three-state model for the SF process to interrogate the relative significance of different factors. By considering a series of three acenes (tetracene, pentacene, and hexacene), we (i) explained the experimentally observed 3 orders of magnitude difference in the rate of SF in tetracene and pentacene, (ii) predicted that the rate of SF in hexacene will be slightly faster than in pentacene. This trend is driven by the increased thermodynamic drive for SF (Gibbs free energy difference of the initial excitonic state and two separated triplets). The important role of entropy was discussed; the anticipated magnitude of entropic contributions was illustrated by simple calculations. The entropy is crucially important; it allows an unfavorable electronic energy difference in tetracene to be overcome. Entropy also facilitates the separation of the two bound triplets (multiexciton state, ^{1}ME) into two independent triplets. The entropy increases both in the first ($S_1 \rightarrow {}^1$ME) and in the second (^{1}ME $\rightarrow 2T_1$) steps. In the former, the entropy increase is due to a delocalized nature of the initial exciton and a localized nature of a multiexciton state (there are multiple ways in which one can chose a dimer from the delocalized exciton). We note that, although completely different in the underlying physics, either delocalization of an excited state in an ordered polycrystalline solid or a high mobility of a localized exciton in disordered solids that enables sampling a certain volume during an exciton's lifetime leads to the same final result in terms of counting microstates in entropy calculations. In the second step, the entropy increases due to multiple possible ways in which the ME state can separate into two triplets. We note that the leading factor in computing these entropic contributions is due to the structure of the respective solids.

We anticipate that in dilute solutions the entropic drive for the first step will not be operational, resulting in a slower kinetics (at least 20−30 times slower) and reduced yields. Thus, in compounds in which SF is endoergic, such as tetracene, SF is expected to be significantly impeded. Pentacene, in which SF is exoergic and does not require additional entropic drive, does exhibit SF in solutions;[28] however, the rate of the multiexciton formation from an excimer-like dimer is 3 orders of magnitude slower than in solid pentacene. We predict that SF is likely to be slow and inefficient in isolated covalently bound dimers of tetracene derivatives, even if the coupling elements are optimized, unless of course the substituents or solvent change the electronic energies of the S_1 and ME states such that the ME state drops below S_1. Low yields (3−5%) and 3 orders of magnitude slower SF rates have been reported for covalently linked tetracene dimers;[27] our model reproduces this trend in the rate.

Another important conclusion is that for an efficient SF, the two thermodynamic quantities, ϵ_b and ϵ_{stt}, may need to be balanced; furthermore, the $r_1(0)$:$r_2(0)$ ratio also affects optimal ϵ_b. We illustrate that under certain conditions there is an optimal relationship between ϵ_b and ϵ_{stt}. For example, for large ϵ_b the first transition (from state 0 to state 1) is faster, while the second transition (from state 1 to state 2) is getting slower, suggesting that there is some optimal value of the multiexciton stabilization energy for a given ϵ_{stt}.

Estimates of optimal ME stabilization energies in the three acenes suggest that their ϵ_b might be too small; thus, the rates of SF in these compounds can be further optimized by designing materials with larger multiexciton stabilization energies. We note that ϵ_b values can be tuned by either electronic or entropic contributions.

Our estimate of the SF rate in DPT is in semiquantitative agreement with the experimental trend. The calculations suggest that the increased efficiency of DPT relative to tetracene is due to the reduced energy gap (E_{stt}).

The model also explains weak temperature dependence[29,30] of the $S_1 \rightarrow$ ME step in tetracene. This is a consequence of a significant entropic drive of this step.

dx.doi.org/10.1021/jp4128176 | J. Phys. Chem. C 2014, 118, 5188−5195

AUTHOR INFORMATION

Corresponding Authors

*E-mail: tolya@rice.edu; 1-713-348-5672.
*E-mail: krylov@usc.edu; 1-213-740-4929.

Notes

The authors declare no competing financial interest.

ACKNOWLEDGMENTS

Support for this work was provided by the Center for Energy Nanoscience, an Energy Frontier Research Center funded by the U.S. Department of Energy, Office of Science, Office of Basic Energy Sciences (DE-SC0001013). A.I.K. also acknowledges support from the Humboldt Research Foundation (Bessel Award). A.B.K. acknowledges the support from the Welch Foundation (grant C-1559). We are grateful to Prof. Sean Roberts (University of Texas, Austin) and Prof. Steve Bradforth (USC) for stimulating discussions, and to Prof. Josef Michl (University of Colorado, Boulder) for his critical feedback about the manuscript.

REFERENCES

(1) Smith, M. B.; Michl, J. Singlet Fission. *Chem. Rev.* **2010**, *110*, 6891−6936.
(2) Singh, S.; Jones, W. J.; Siebrand, W.; Stoicheff, B. P.; Schneider, W. G. Laser Generation of Excitons and Fluorescence in Anthracene Crystals. *J. Chem. Phys.* **1965**, *42*, 330−342.
(3) Smith, M. B.; Michl, J. Recent Advances in Singlet Fission. *Annu. Rev. Phys. Chem.* **2013**, *64*, 361−368.
(4) Johnson, J. C.; Nozik, A. J.; Michl, J. The Role of Chromophore Coupling in Singlet Fission. *Acc. Chem. Res.* **2013**, *46*, 1290−1299.
(5) Zimmerman, P. M.; Musgrave, C. B.; Head-Gordon, M. A Correlated Electron View of Singlet Fission. *Acc. Chem. Res.* **2012**, *46*, 1339−1347.
(6) Kuhlman, T. S.; Kongsted, J.; Mikkelsen, K. V.; Møller, K. B.; Sølling, T. I. Interpretation of the Ultrafast Photoinduced Processes in Pentacene Thin Films. *J. Am. Chem. Soc.* **201o**, *132*, 3431−3439.
(7) Zimmerman, P. M.; Bell, F.; Casanova, D.; Head-Gordon, M. Mechanism for Singlet Fission in Pentacene and Tetracene: From Single Exciton to Two Triplets. *J. Am. Chem. Soc.* **2011**, *133*, 19944−19952.
(8) Darancet, S.; Sharifzadeh, P.; Kronik, L.; Neaton, J. B. Low-Energy Charge-Transfer Excitons in Organic Solids from First-Principles: The Case of Pentacene. *J. Phys Chem. Lett.* **2013**, *4*, 2917−2201.
(9) Havenith, R. W. A.; de Gier, H. D.; Broer, R. Explorative Computational Study of the Singlet Fission Process. *Mol. Phys.* **2012**, *110*, 2445−2454.
(10) Congreve, D. N.; Lee, J.; Thompson, N. J.; Hontz, E.; Yost, S. R.; Reusswig, P. D.; Bahlke, M. E.; Reineke, S.; Van Voorhis, T.; Baldo, M. A. External Quantum Efficiency Above 100% in a Singlet-Exciton-Fission Based Organic Photovoltaic Cell. *Science* **2013**, *340*, 334−337.
(11) Vallett, P. J.; Snyder, J. L.; Damrauer, N. H. Tunable Electronic Coupling and Driving Force in Structurally Well Defined Tetracene Dimers for Molecular Singlet Fission: A Computational Exploration Using Density Functional Theory. *J. Phys. Chem. A* **2013**, *117*, 10824−10838.
(12) Casanova, D. Electronic Structure Study of Singlet-Fission in Tetracene Derivatives. *J. Chem. Theory Comput.* **2013**, *10*, 324−334.
(13) Feng, X.; Luzanov, A. V.; Krylov, A. I. Fission of Entangled Spins: An Electronic Structure Perspective. *J. Phys. Chem. Lett.* **2013**, *4*, 3845−3852.
(14) Mou, W.; Hattori, S.; Rajak, P.; Shimojo, F.; Nakano, A. Nanoscopic Mechanisms of Singlet Fission in Amorphous Molecular Solid. *Appl. Phys. Lett.* **2013**, *102*, 173301.
(15) Berkelbach, T. C.; Hybertsen, M. S.; Reichman, D. R. Microscopic Theory of Singlet Exciton Fission. I. General Formulation. *J. Chem. Phys.* **2012**, *138*, 114102.
(16) Chan, W.-L.; Ligges, M.; Zhu, X.-Y. The Energy Barrier in Singlet Fission Can Be Overcome through Coherent Coupling and Entropic Gain. *Nat. Chem.* **2012**, *4*, 840−845.
(17) Suna, A. Kinematics of Exciton-Exciton Annihilation in Molecular Crystals. *Phys. Rev. B* **1970**, *1*, 1716−1739.
(18) Johnson, R. C.; Merrifield, R. E. Effects of Magnetic Fields on the Mutual Annihilation of Triplet Excitons in Anthracene Crystals. *Phys. Rev. B* **1970**, *1*, 896−902.
(19) Roberts, S. T.; McAnally, R. E.; Mastron, J. N.; Webber, D. H.; Whited, M. T.; Brutchey, R. L.; Thompson, M. E.; Bradforth, S. E. Efficient Singlet Fission Found in a Disordered Acene Film. *J. Am. Chem. Soc.* **2012**, *134*, 6388−6400.
(20) Piland, G. B.; Burdett, J. J.; Kurunthu, D.; Bardeen, C. J. Magnetic Field Effects on Singlet Fission and Fluorescence Decay Dynamics in Amorphous Rubrene. *J. Phys. Chem. C* **2013**, *117*, 1224−1236.
(21) Whitten, W. B.; Arnold, S. Pressure Modulation of Exciton Fission in Tetracene. *Phys. Status Solidi* **1976**, *74*, 401−407.
(22) Lee, J.; Jadhav, P.; Reusswig, P. D.; Yost, S. R.; Thompson, N. J.; Congreve, D. N.; Hontz, E.; Van Voorhis, T.; Baldo, M. A. Singlet Exciton Fission Photovoltaics. *Acc. Chem. Res.* **2013**, *46*, 1300−1311.
(23) Angliker, H.; Rommel, E.; Wirz, J. Electronic Spectra of Hexacene in Solution. *Chem. Phys. Lett.* **1982**, *87*, 208−212.
(24) Watanabe, M.; Chang, Y.; Liu, S.; Chao, T.; Goto, K.; Islam, M. M.; Yuan, C.; Tao, Y.; Shinmyozu, T.; Chow, T. J. The Synthesis, Crystal Structure and Chargetransport Properties of Hexacene. *Nat. Chem.* **2012**, *4*, 574−578.
(25) Anslyn, E. V.; Dougherty, D. A. *Modern Physical Organic Chemistry*; University Science Books: Herndon, VA, 2006.
(26) vanKampen, N. G. *Stochastic Processes in Physics and Chemistry*, 2nd ed.; Elsevier: New York, 2001.
(27) Burdett, J. J.; Bardeen, C. J. The Dynamics of Singlet Fission in Crystalline Tetracene and Covalent Analogues. *Acc. Chem. Res.* **2013**, *46*, 1312−1320.
(28) Walker, B. J.; Musser, A. J.; Beljonne, D.; Friend, R. H. Singlet Exciton Fission in Solution. *Nat. Chem.* **2013**, *5*, 1019−1024.
(29) Burdett, J. J.; Gosztola, D.; Bardeen, C. J. The Dependence of Singlet Exciton Relaxation on Excitation Density and Temperature in Polycrystalline Tetracene Thin Films: Kinetic Evidence for a Dark Intermediate State and Implications for Singlet Fission. *J. Chem. Phys.* **2011**, *135*, 214508.
(30) Wilson, M. W. B.; Rao, A.; Johnson, K.; Gélinas, S.; di Pietro, R.; Clark, J.; Friend, R. H. Temperature-Independent Singlet Exciton Fission in Tetracene. *J. Am. Chem. Soc.* **2013**, *135*, 16680−16688.
(31) Burdett, J. J.; Müller, A. M.; Gosztola, D.; Bardeen, C. J. Excited State Dynamics in Solid and Monomeric Tetracene: The Roles of Superradiance and Exciton Fission. *J. Chem. Phys.* **2010**, *133*, 144506.